Original Article

Molecular Interaction Of Acetyl-Coa Carboxylase (Accase) With Fenoxaprop-P Ethyl Through Computational Analysis

Muhammad Moazzam Bin Rasheed*[1] , Mian Talha Sarfraz[2] , Marvah Mehmood Rana[3] , Muhammad Hassan Taj[4] , Sana Shamim[5] , Sadaf Ibrahim[6] , Noor Jahan[7] , Muhammad Ameer Moaavia[8]

[1]ranamoazzamuaf@gmail.com
[2]talhasarfraz29@gmail.com
[3]marvahmahmood@gmail.com
[4]Hassan.84np@gmail.com
[5]Sana.shamim@duhs.edu.pk
[6]Sadaf. Ibrahim@zu.edu.pk
[7]Noor.jahan@duhs.edu.pk
[8]Ameermoaavia17@gmail.com

1) CABB department University of Agriculture Faisalabad Pakistan
2,3) School of Interdisciplinary Engineering & Science (SINES), NUST, Islamabad
4) University of Agriculture Faisalabad, Pakistan
5,7) Department of Pharmaceutical Chemistry, Dow College of Pharmacy, faculty of Pharmaceutical Sciences, Dow university of health Sciences
6) Department of pharmacology, faculty of pharmacy, ziauddin University
8) University of Lahore
*Correspondence
ranamoazzamuaf@gmail.com
DOI: 10.47750/pnr.2023.14.04.67

Abstract

Herbicides are critical in preventing crop production losses in no-till systems because of their weed-control capabilities as well as their ability to preserve rising soil. Weed resistance to herbicides must be reduced because it is a critical control feature on behalf of diet security. Cross resistance may happen through herbicides from very similar or diverse herbicide families, as well as beside the similar or dissimilar site of action. Weed struggle in the direction of herbicides must be reduced since it is a critical control feature designed for diet protection. The objective of research to determine the enzyme ACCase interaction with the fenoxaprop-p-ethyl as a protein ligand interaction and Molecular dynamics MD simulation analysis to confirm the physical movement of atoms and molecule. Various computational methods and tools were used to find out interaction i.e., RCSB PDB, PubChem, MGL Auto dock vina, Discovery studio, UCSF Chimera, Desmond Schrodinger, and Maestro Schrodinger. The result was concluded that herbicide protein binds to the active site on the receptor at specific location. The 3jzf protein bind with the ARG_292 and make good interaction, the HIS_209 make Hydrophobic bond, GLN_233 and GLN_237 make good hydrogen bond and HIS_236 make water bridges. These residues make excellent interaction with the surrounding residues in 3jzf protein with the ligand Fenoxaprop-p ethyl, ASP_382 is the most important ones in terms of H-bonds for (3jzi) that is not stable bonding. The complex 3jzf indicates that the complex reaches stability at 5 ns and remained stable till 35 ns after that there was a little increase in RMD of ligand but again it becomes stable with protein. The complexity of the RMSD plot for the given 3jzi shows that it achieves stabilization about 30 ns. However, the RMSD for the ligand is quite high, indicating a poor interaction. After then, an overall RMSD value of 2.0 Å, for (3jzf) and 3.0 Å, for (3jzi) remains for ligand up to 50 ns. After becoming stable, protein RMSD values vary within 1.0 Angstrom. This indicates that the ligand stayed attached to the receptor'sbinding site for most of the simulated time. However, there is greater variation in (3jzi) than in (3jzf). Molecular docking modeling show and verify that protein and ligand have the similar relations beside nearby residues, resulting in an outstanding match through ACCase' active site.

Key Words Acetyl-CoA carboxylase, Fenoxaprop-p ethyl, computational analysis.

Introduction

Acetyl-CoA carboxylase (ACCase - EC 6.4.1.2) inhibitors was utilized on large scale at the start of 1980's. They are class of herbicides which were found as most recognized cases of resistance (Moss, 2002). Herbicide-

resistance procedure largely has two classifications: target-site mechanisms and non-target-site mechanisms (Powles et al., 2010; Délye et al., 2013). Target-site mechanism modification at molecular target of the herbicide (usually an enzyme) which decrease herbicide efficacy. However, most target-site resistance could be happened at specific target, which results inborne herbicide essential for achieving a lethal effect (Laforest et al., 2017; Gaines et al., 2010). Non-target-site resistance incorporate with target site resistance can have more chances of resistance against particular herbicide.

The chances of mutation on DNA are not happen or very low leads to non-target-site resistance. (Délye,2013) Comparatively, the first DNA change progressed to target-site resistance (to triazines) was observed over three to five years ago (Hirschberg, Mcintosh,1983). The enzyme acetyl-CoA carboxylase (ACCase, EC 6.4.1.2) is responsible for the first and most essential step in fatty acid biosynthesis (are found in all biological species) (Huerlimann and Heimann, 2013; Keereetaweep et al., 2018).

To maintain cell functions, ACCase catalyzes the development of malonyl-CoA, a key component in the biosynthesis of long-chain fatty acids (Yang et al., 2018; Joyard et al., 2010;). Beginning with acetyl-CoA and CO2, the formation of Malonyl CoA is generated in two phases. ACCase's vitamin H carboxylase subunit first catalyzes ATP dependent on vitamin H carboxylation. The carboxyl transferase subunit then catalyzes the transfer of an active carboxyl group to acetyl-CoA, its acceptor. (Xiang et al., 2009).

Once ACCase is repressed, the developed plants bleach and ultimately endures necrosis leads to death. Herbicides containing the advantages of ACCase include a large weed-control area, ease of use, and low cost a long-lasting application time and strong herbicide compatibility. (Tehranchian et al., 2017; Lancaster et al., 2018; Powles, 2005). Though, there has been a rise in grass weed conflict as a result of the widespread use of this class of herbicides. (Mccullough et al., 2017; Saini et al., 2017; Laforest et al., 2017).

Fenoxaprop-P-ethyl is a contact and systemically absorbed selective herbicide with translocation to roots or rhizomes, both acropetally and basipetally. It inhibits production of fatty acids. Annual grass weeds and wild oats are controlled after emergence in rice, wheat, rye, barley, oat, and triticale. Fenoxaprop-p-ethyl is absorbed and systemically translocated by plant leaves and stems. It inhibits most of the production of fatty acids in grassy weeds meri- stem tissue.

Computational biology makes easy to find different problem on virtual bases and provide ease in designing experiment instead of laborious and testable initial wet lab experiments **(**Markowetz, 2017). Docking techniques are widely used to detect drug-like molecules. It acts together with a given receptor to prevent its function. Even though receptors are identified to change configuration upon ligand binding. Furthermost, docking programs is so flexible which provide interaction of typical small fragments as well as rigid modeling receptors. The main objective of this research to determine the enzyme ACCase interaction with the fenoxaprop-p-ethyl as a protein ligand interaction and Molecular dynamics MD simulation analysis to confirm the physical movement of atoms and molecule. Molecular docking modeling show and verify that protein and ligand have the similar relations beside nearby residues, resulting in an outstanding match through ACCase active site. this research strengthens the strategies development at molecular level to control the weedicide at early.

The basic aim and objective of this study were that:

- To determine the enzyme ACCase (3jzf and 3jzi) interaction with the fenoxaprop-p- ethyl as a protein ligand interaction.
- To do Molecular dynamics MD simulation analysis to confirm the physical movement of atoms and molecule.

Methodology

Research conducted in plant stress lab at CABB University of Agriculture Faisalabad. Research work done by using bioinformatics tools to find out protein ligand interaction.

Retrieval of Data:

The desired protein of ACCase (PDB ID: 3JZF and PDB ID: 3JZI) retrieved from Protein data bank (PDB) database and ligand fenoxaprop-p-ethyl (Compound CID: 91707) retrieved from PubChem database and constructed their 2D and 3D structures. For protein purification removed the water molecules from the protein and polar the hydrogen bond.

Protein structure (Acetyl-CoA- Carboxylase (ACCase):

The structure of ACCase proteins (3jzf and 3jzi) used as protein in current study was generated through Discovery Studio and Chimera. The 2D and 3D view of proteins was established to get better interaction with ligand (Fenoxaprop-P-ethyl.

The grid parameter file specifies which receptor the potentials should be computed around, the types of maps to be computed, and the location and extent of those maps.

Confirmation of protein ligand interaction analysis:

Molecular analysis performed to confirm the desired protein ligand interaction by different tools like MGL Autodock vina, Desmond, Maestro, discovery studio and UCSF Chimera. These tools will be used for the molecular docking, simulation and visualization of the protein that bind to the active site of the receptor and then the Ramachandran plot will be constructed for self-homology.

Molecular Dynamics Simulation

Desmond, a package from Schrödinger LLC, was used to run molecular dynamics simulations for 50 nanoseconds. Docking experiments provided the earliest step of protein and ligand complexes for molecular dynamics modelling. In static circumstances, Molecular Docking Studies provide a forecast of ligand binding state. To anticipate the ligand binding status in the physiological milieu, simulations were run. Protein Preparation Wizard or Maestro were used to prepare protein–ligand complexes, which consist of complex optimize and minimization. The System Builder tool was used to prepare all systems. TIP3P, a liquid type with an orthorhombic structure, was chosen (Transferable Intermolecular Interaction Potential 3 Points). The OPLS 2005 influence field continued to be used in the simulation. Counter ions occurred used to neutralize the models when needed. 0.15 M salt (NaCl) was added to simulate physiological circumstances. For the whole simulation, The NPT ensembles were employed, with a temperature of 300 K and a force of 1 atm. The models were relaxed prior to the simulation. The paths were saved each 100 ps intended for analysis, and the simulation's stability was verified by monitoring the protein and ligand's root mean square deviation (RMSD) across time.

The Desmond simulation's pathways were investigated. The root mean square deviation (RMSD), root mean square fluctuation (RMSF), and protein–ligand interactions were calculated using MD trajectory analysis.

Visualization of binding conformations and Docking analysis:

Iterated local search approach depending on the search space parameters provided by Auto Dock Vina, was utilized for docking analysis. As a result, binding energies (Kcal/mol) and optimal binding conformations were determined.

Evaluate the docking and simulation confirmation process by following protocol:

1. Perform redocking or self-docking and cross docking simulation.
2. Computing the relative docking accuracies based on root mean square deviation (RMSD) values between the predicted (docked) and experimental binding poses

This protocol is characterized by four steps:

1. Setup working Directories.
2. Preparation the structure and input files.
3. Docking Simulation, cluster analysis, and DA Analysis.

4. Analysis and verify the results.

In Discovery Studio and chimera, the binding conformations with the lowest energy coefficients were chosen and displayed. Using linear (2D) and spatial (3D) and interaction maps, the amino acids involved around ligand-protein interactions were identified.

Results

Simulation Interactions of 3jzf and 3jzi

Simulation Details for 3jzf

Desmond, a package from Schrödinger LLC, was used to run molecular dynamics simulations for 50 nanoseconds. Docking experiments provided the earliest step of protein and ligand complexes for molecular dynamics modelling.

Jobname: 3jzf-fpe
Entry title: Full System

CPU #	Job Type	Ensemble	Temp. [K]	Sim. Time [ns]	# Atoms	# Waters	Charge
1	mdsim	NPT	300.0	50.098	35963	9991	0

Protein Information

Tot. Residues	Prot. Chain(s)	Res. in Chain(s)	# Atoms	# Heavy Atoms	Charge
380	'A'	ict_values([380]	5892	2933	-1

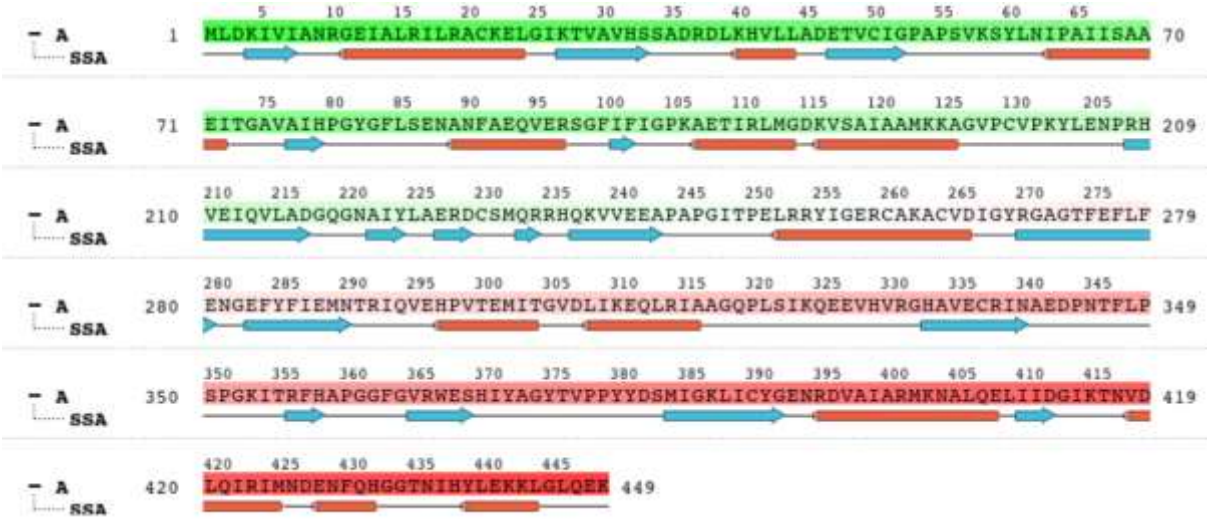

Ligand Information

SMILES	CCOC(=O)[C@@H](C)Oc1ccc(cc1)Oc(n2)oc(c23)cc(Cl)cc3
PDB Name	'UNK'
Num. of Atoms	41 (total) 25 (heavy)
Atomic Mass	361.785 au
Charge	0
Mol. Formula	C18H16ClNO5
Num. of Fragments	5
Num. of Rot. Bonds	7

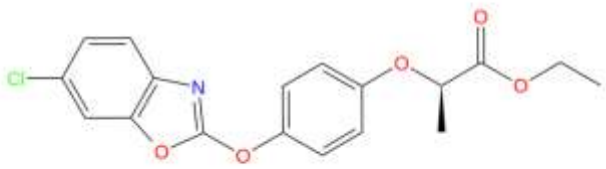

Counter Ion/Salt Information

Type	Num.	Concentration [mM]	Total Charge
Na	29	52.775	+29
Cl	28	50.955	-28

Simulation Details for 3jzi

Desmond, a package from Schrödinger LLC, was used to run molecular dynamics simulations for 50 nanoseconds. Docking experiments provided the earliest step of protein and ligand complexes for molecular dynamics modelling.

Tot. Residues	Prot. Chain(s)	Res. in Chain(s)	# Atoms	# Heavy Atoms	Charge
445	'A'	ict_values([445]	6755	3376	-4

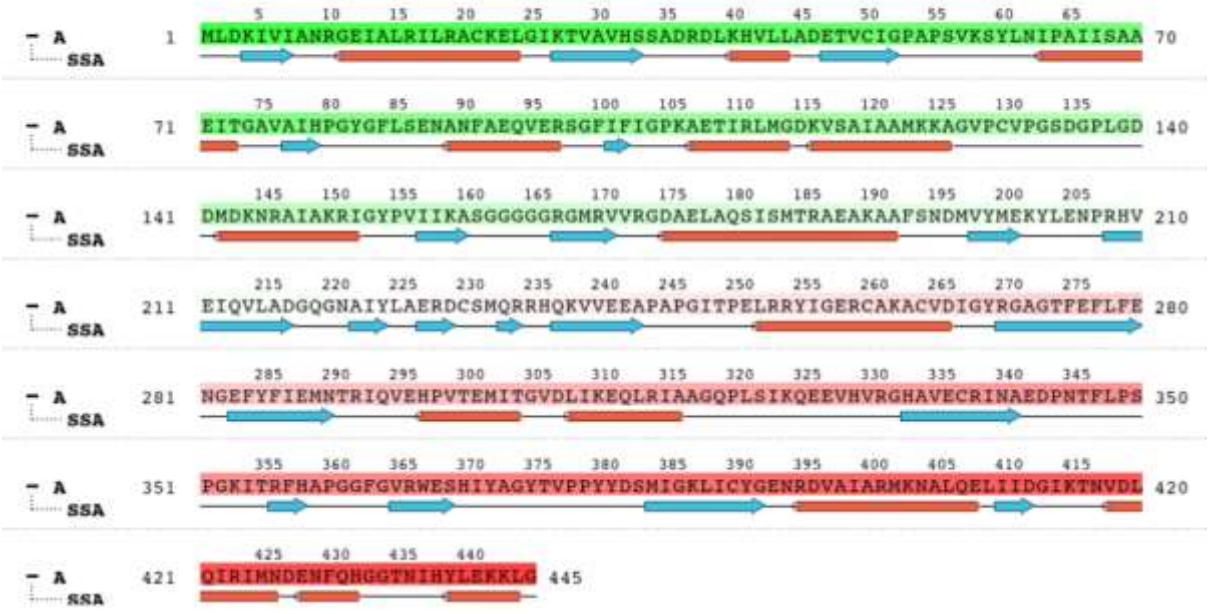

Ligand Information

SMILES	CCOC(=O)[C@@H](C)Oc1ccc(cc1)Oc(n2)oc(c23)cc(Cl)cc3
PDB Name	'UNK'
Num. of Atoms	41 (total) 25 (heavy)
Atomic Mass	361.785 au
Charge	0
Mol. Formula	C18H16ClNO5
Num. of Fragments	5
Num. of Rot. Bonds	7

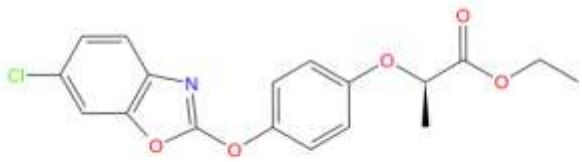

Counter Ion/Salt Information

Type	Num.	Concentration [mM]	Total Charge
Na	38	57.247	+38
Cl	34	51.221	-34

Diagrammatically illustration of 3jzf and 3jzi protein ligand view in discovery studio are following below:

Result of protein binding with ligand in the discovery studio.

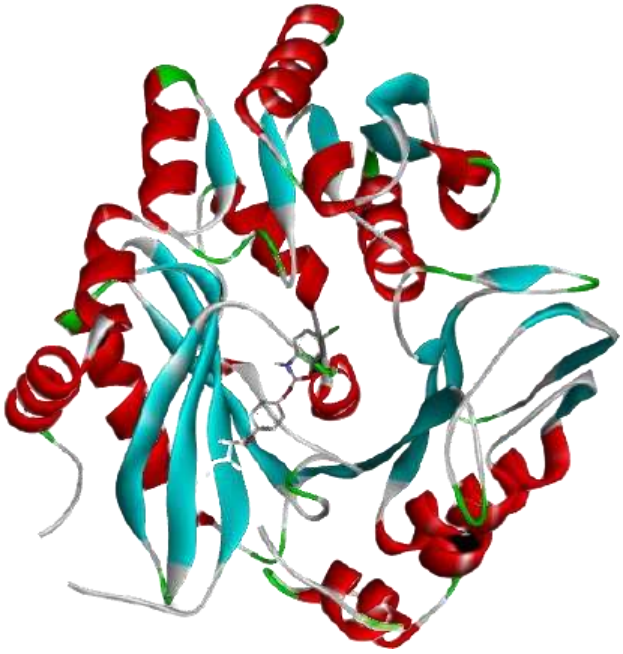

Fig 4.23. 3D purified protein ligand binding view of 3jzf

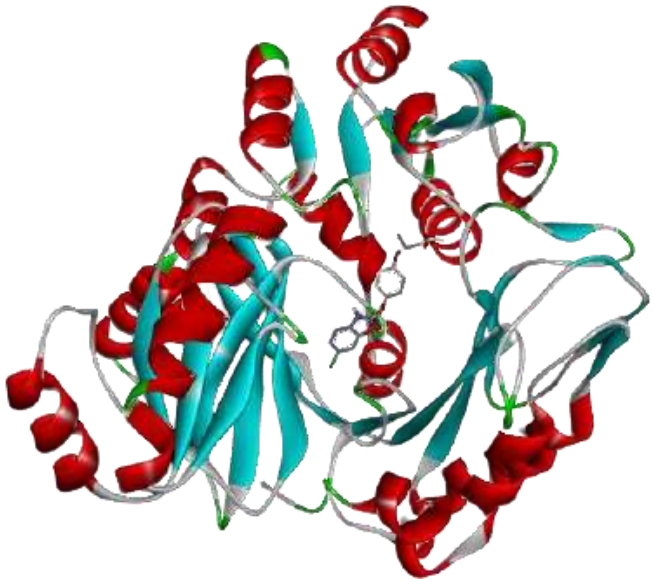

Fig 4.24. Purified 3D protein ligand binding view of 3jzi

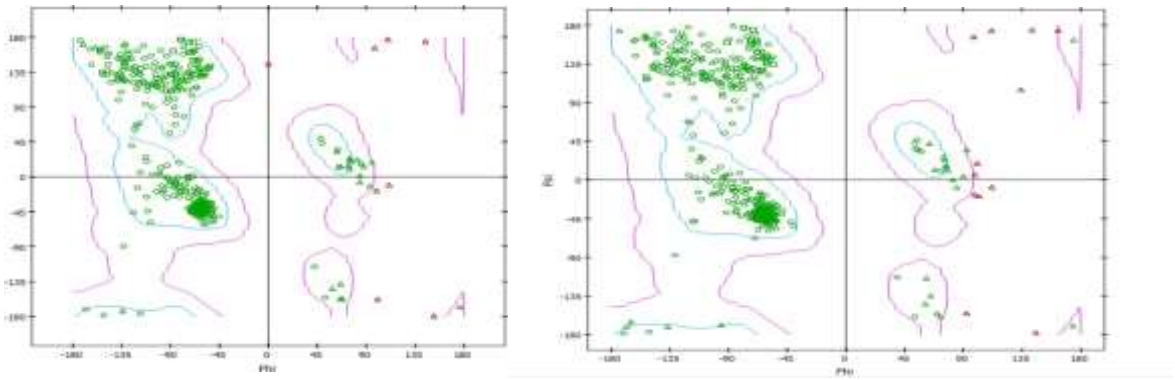

Fig 4.31, 4.32 In the given diagrams of the Ramachandran plot for 3jzi and 3jzf protein ligan.

This shows the distribution of statistical combinations, also used for self-homology

Protein-Ligand RMSD

Root mean square fluctuation (RMSF), and protein–ligand contacts were calculated from MD trajectory analysis.

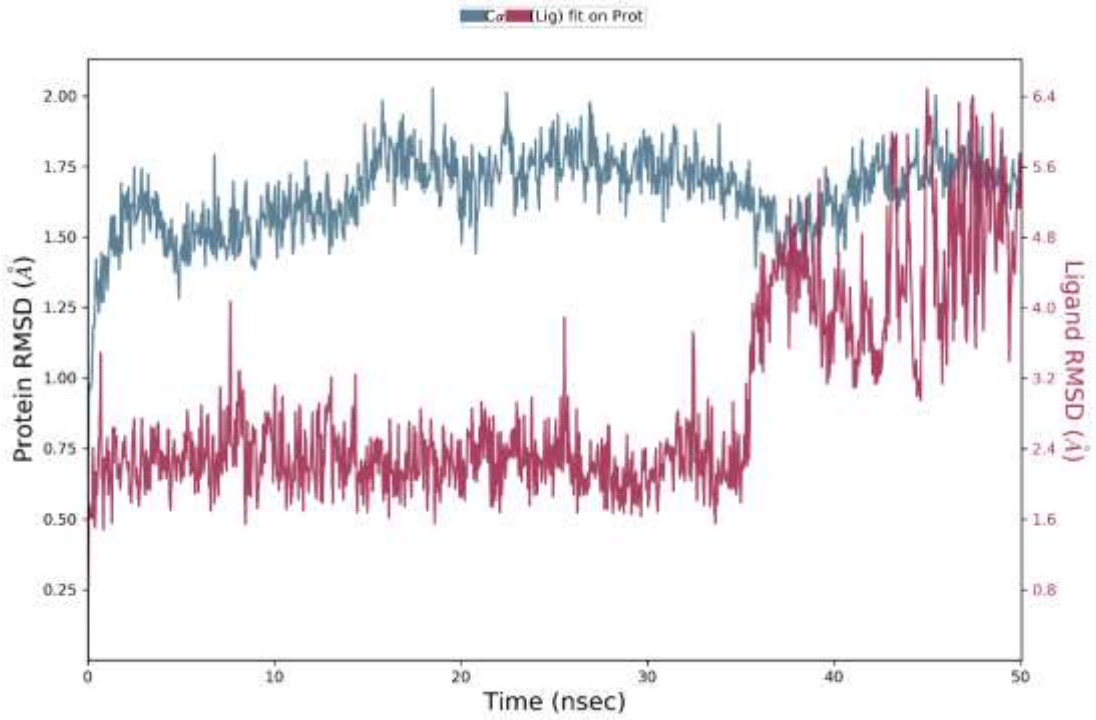

Figure 1: Root mean square deviation (RMSD) of the C-alpha atoms of protein (3jzf) and the ligand with time. The left Y-axis shows the variation of protein RMSD through time. The right Y-axis shows the variation of ligand RMSD through time.

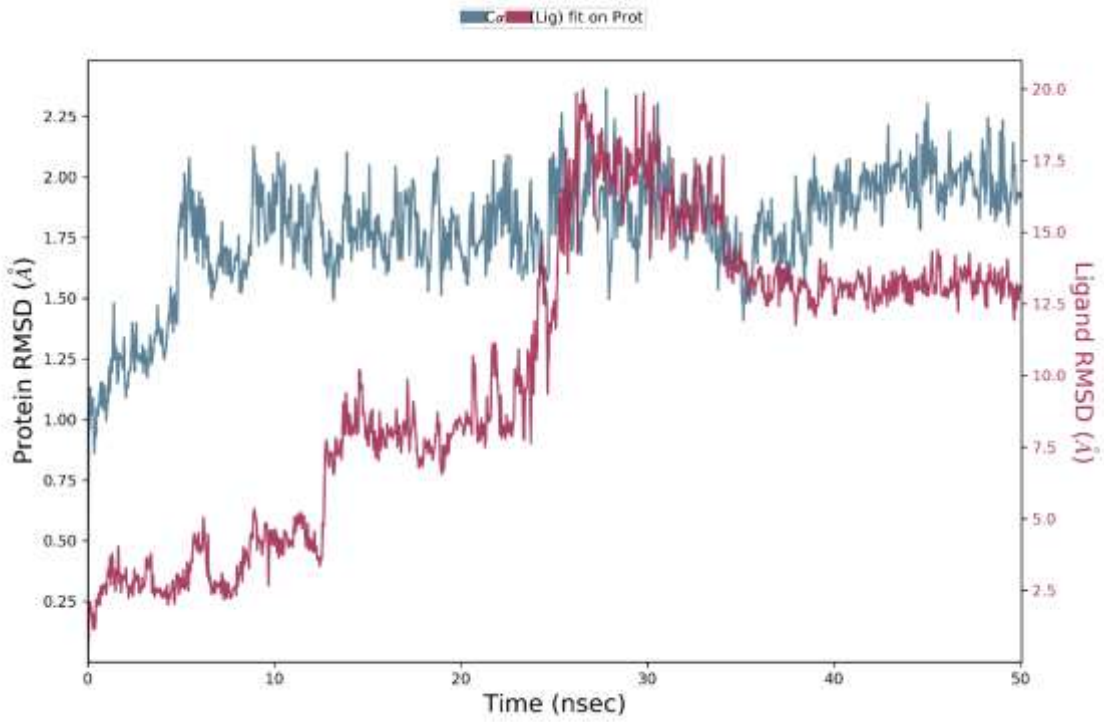

Figure 2: Root mean square deviation (RMSD) of the C-alpha atoms of protein (3jzi) and the ligand with time. The left Y-axis shows the variation of protein RMSD through time. The right Y-axis shows the variation of ligand RMSD through time.

The Root Mean Square Deviation (RMSD) is used to measure the average change in displacement of a selection of atoms for a particular frame with respect to a reference frame. It is calculated for all frames in the trajectory. The RMSD for frame x is:

$$RMSD_x = \sqrt{\frac{1}{N}\sum_{i=1}^{N}(r_i'(t_x)) - r_i(t_{ref}))^2}$$

where N is the number of atoms in the atom selection; t_{ref} is the reference time, (typically the first frame is used as the reference and it is regarded as time t=0); and r' is the position of the selected atoms in frame x

after superimposing on the reference frame, where frame x is recorded at time t_x. The procedure is repeated for every frame in the simulation trajectory.

Protein RMSD

The above plot shows the RMSD evolution of a protein (left Y-axis). All protein frames are first aligned on the reference frame backbone, and then the RMSD is calculated based on the atom selection.

Monitoring the RMSD of the protein can give insights into its structural conformation throughout the simulation. RMSD analysis can indicate if the simulation has equilibrated — its fluctuations towards the end of the simulation are around some thermal average structure. Changes of the order of 1-3 Å are perfectly acceptable for small, globular proteins. Changes much larger than that, however, indicate that the protein is undergoing a large conformational change during the simulation. It is also important that your simulation converges — the RMSD values stabilize around a fixed value. If the RMSD of the protein is still increasing or decreasing on average at the end of the simulation, then your system has not equilibrated, and your simulation may not be long enough for rigorous analysis.

Ligand RMSD

Ligand RMSD (right Y-axis) indicates how stable the ligand is with respect to the protein and its binding pocket. In the above plot, 'Lig fit Prot' shows the RMSD of a ligand when the protein-ligand complex is first aligned on the protein backbone of the reference and then the RMSD of the ligand heavy atoms is measured. If the values observed are significantly larger than the RMSD of the protein, then it is likely that the ligand has diffused away from its initial binding site.

Figure 1 & 2 show the evolution of RMSD values in the course of time for the C-alpha atoms of the ligand bound protein. The RMSD plot of the complex 3jzf indicates that the complex reaches stability at 5 ns and remained stable till 35 ns after that there was a little increase in RMD of ligand but again it becomes stable with protein. The RMSD plot of the complex 3zfi indicates that the complex reaches stability at 30 ns. But the RMSD for ligand is very high which shows its poor interaction. From then, an average RMSD value of 2.0 Å for (3jzf) and 3.0 Å for (3jzi) persists up to 50 ns for ligand. Protein RMSD values fluctuates within 1.0 Angstrom after being stable. These indicate that the ligand remained bound to the binding site of the receptor during most of the simulation period. However, there is more deviation in (3jzi) as compared to (3jzf).

Protein RMSF

Figure 3 & 4 show the residue wise RMSF value of the protein bound to the ligand. The residues showing higher peaks correspond to loop regions, as identified from MD trajectories (Figure 5 & 6), or N and C-terminal zones. Low RMSF values of binding site residues indicate the stability of ligand binding to the protein.

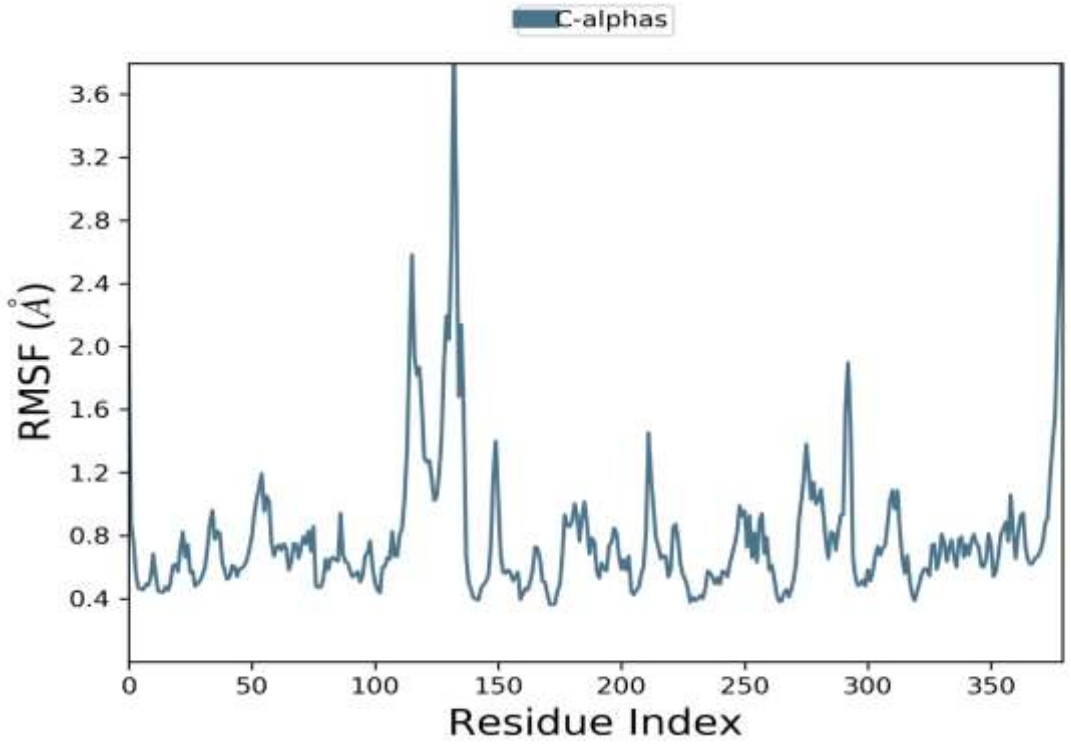

Figure 3: Residue wise Root Mean Square Fluctuation (RMSF) of protein (3jzf).

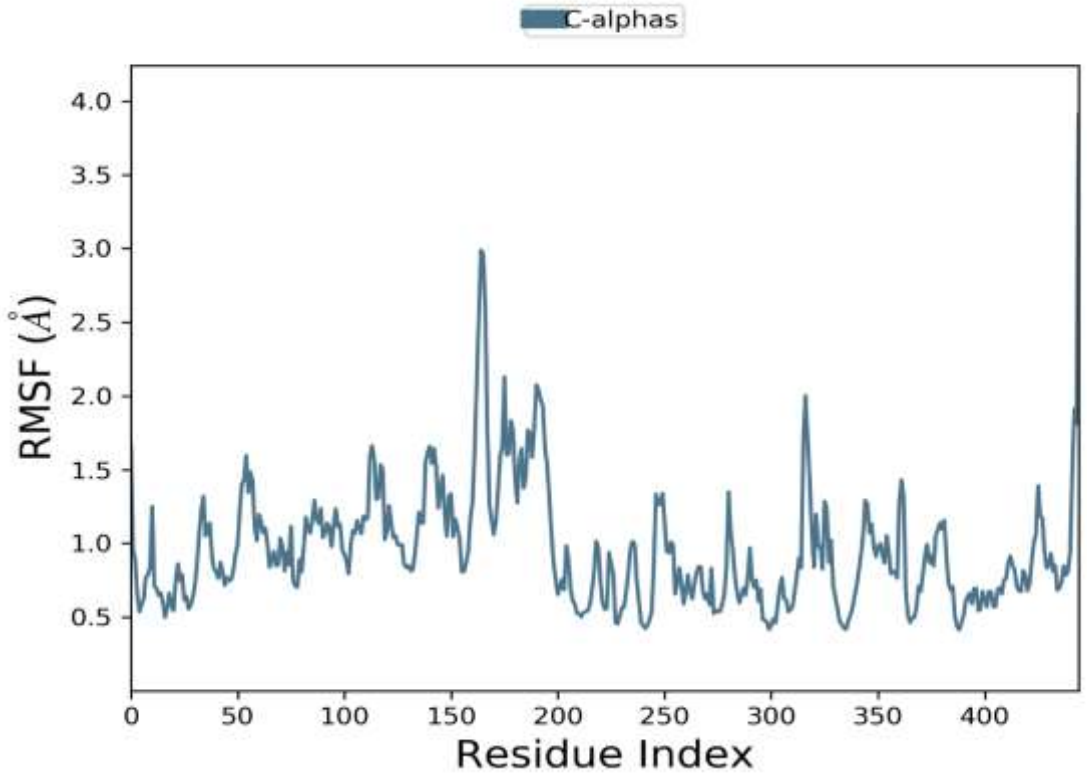

Figure 4: Residue wise Root Mean Square Fluctuation (RMSF) of protein (3jzi).

The Root Mean Square Fluctuation (RMSF) is useful for characterizing local changes along the protein chain. The RMSF for residue i is:

$$RMSF_i = \sqrt{\frac{1}{T}\sum_{t=1}^{T} < (r_i'(t)) - r_i(t_{ref}))^2 >}$$

where T is the trajectory time over which the RMSF is calculated, t_{ref} is the reference time, r_i is the position of residue i; r' is the position of atoms in residue i after superposition on the reference, and the angle brackets

indicate that the average of the square distance is taken over the selection of atoms in the residue.

On this plot, peaks indicate areas of the protein that fluctuate the most during the simulation. Typically, you will observe that the tails (N- and C-terminal) fluctuate more than any other part of the protein. Secondary structure elements like alpha helices and beta strands are usually more rigid than the unstructured part of the protein, and thus fluctuate less than the loop regions. Protein Secondary Structure

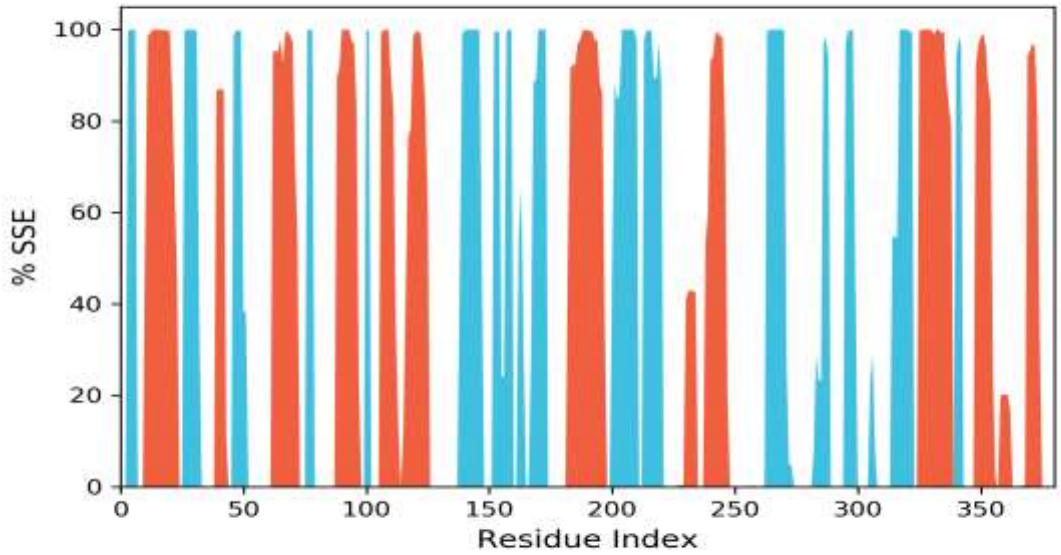

Figure 5: Protein Secondary Structure element distribution by residue index throughout the protein structure (3jzf). Red columns indicate alpha helices, and blue columns indicate beta-strands.

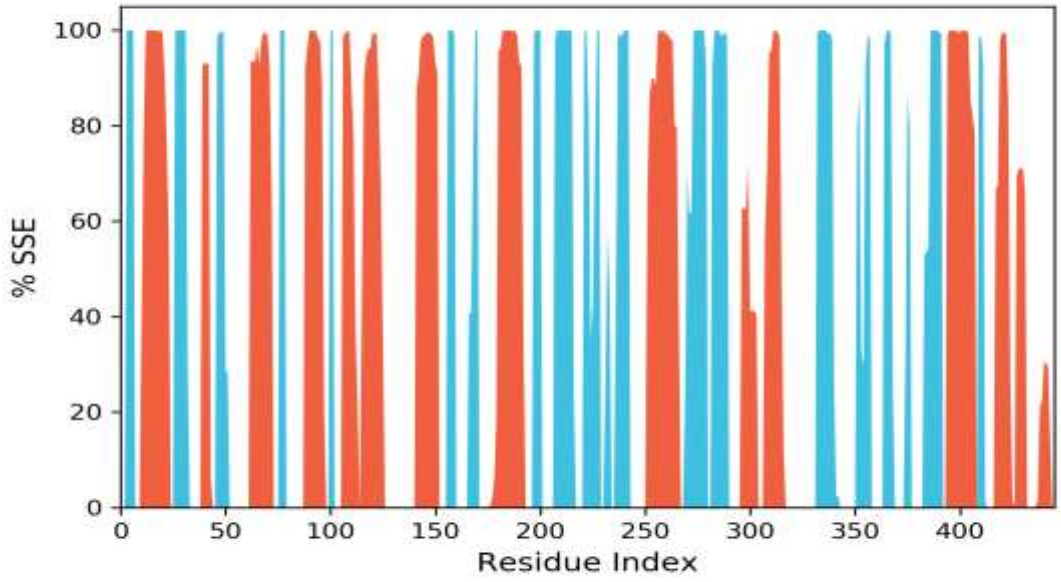

Figure 6: Protein Secondary Structure element distribution by residue index throughout the protein structure (3jzi). Red columns indicate alpha helices, and blue columns indicate beta-strands.

Protein secondary structure elements (SSE) like alpha-helices and beta-strands are monitored throughout the simulation. The plot above reports SSE distribution by residue index throughout the protein structure. The plot below summarizes the SSE composition for each trajectory frame over the course of the simulation, and the plot at the bottom monitors each residue and its SSE assignment over time.

Protein-Ligand Contacts

Protein interactions with the ligand can be monitored throughout the simulation. These interactions can be categorized by type and summarized, as shown in the plot above. Protein-ligand interactions (or 'contacts') are categorized into four types: Hydrogen Bonds, Hydrophobic, Ionic and Water Bridges. Each interaction type contains more specific subtypes, which can be explored through the 'Simulation Interactions Diagram' panel. The stacked bar charts are normalized over the course of the trajectory: for example, a value of 0.7 suggests that 70% of the simulation time the specific interaction is maintained. Values over 1.0 are possible as some protein residue may make multiple contacts of same subtype with the ligand.

Hydrogen Bonds: (H-bonds) play a significant role in ligand binding. Consideration of hydrogen-bonding properties in drug design is important because of their strong influence on drug specificity, metabolization and adsorption. Hydrogen bonds between a protein and a ligand can be further broken down into four subtypes: backbone acceptor; backbone donor; side-chain acceptor; side-chain donor.

The current geometric criteria for protein-ligand H-bond is: distance of 2.5 Å between the donor and acceptor atoms (D—H···A); a donor angle of $^{3}120°$ between the donor-hydrogen-acceptor atoms (D—H···A); and an acceptor angle of $^{3}90°$ between the hydrogen-acceptor-bonded atom atoms (H···A—X).

Hydrophobic contacts: fall into three subtypes: p-Cation; p-p; and Other, non-specific interactions. Generally, these type of interactions involve a hydrophobic amino acid and an aromatic or aliphatic group on the ligand, but we have extended this category to also include p-Cation interactions.

The current geometric criteria for hydrophobic interactions is as follows: p-Cation — Aromatic and charged groups within 4.5 Å; p-p — Two aromatic groups stacked face-to-face or face-to-edge; Other — A non-specific hydrophobic sidechain within 3.6 Å of a ligand's aromatic or aliphatic carbons.

Ionic interactions: or polar interactions, are between two oppositely charged atoms that are within 3.7 Å of each other and do not involve a hydrogen bond. We also monitor Protein-Metal-Ligand interactions, which are defined by a metal ion coordinated within 3.4 Å of protein's and ligand's heavy atoms (except carbon). All ionic interactions are broken down into two subtypes: those mediated by a protein backbone or side chains.

Water Bridges: are hydrogen-bonded protein-ligand interactions mediated by a water molecule. The hydrogen-bond geometry is slightly relaxed from the standard H-bond definition.

The current geometric criteria for a protein-water or water-ligand H-bond are: a distance of 2.8 Å between the donor and acceptor atoms (D—H···A); a donor angle of $^{3}110°$ between the donor-hydrogen-acceptor atoms (D—H···A); and an acceptor angle of $^{3}90°$ between the hydrogen-acceptor-bonded_atom atoms (H···A—X).

Most of the important interactions of ligand–proteins determined with MD are hydrogen bonds and hydrophobic interactions, as depicted in Figure 7 & 8. GLN_233 and GLN_237 are the most important ones in terms of H-bonds for (3jzf). ASP_382 is the most important ones in terms of H-bonds for (3jzi). The stacked bar charts were normalized over the course of the trajectory: for example, a value of 1.0 suggests that for 100% of the simulation time, the specific interaction was maintained. Values over 1.0 are possible as some protein residue may make multiple contacts of the same subtype with the ligand.

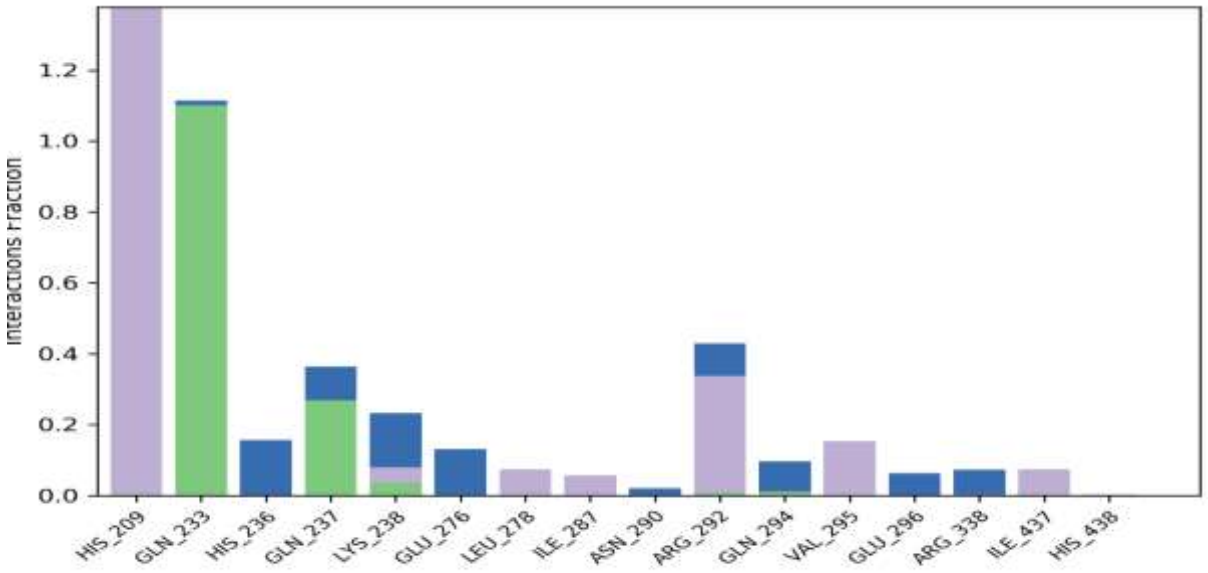

Figure 7: Protein-ligand contact histogram (3jzf).

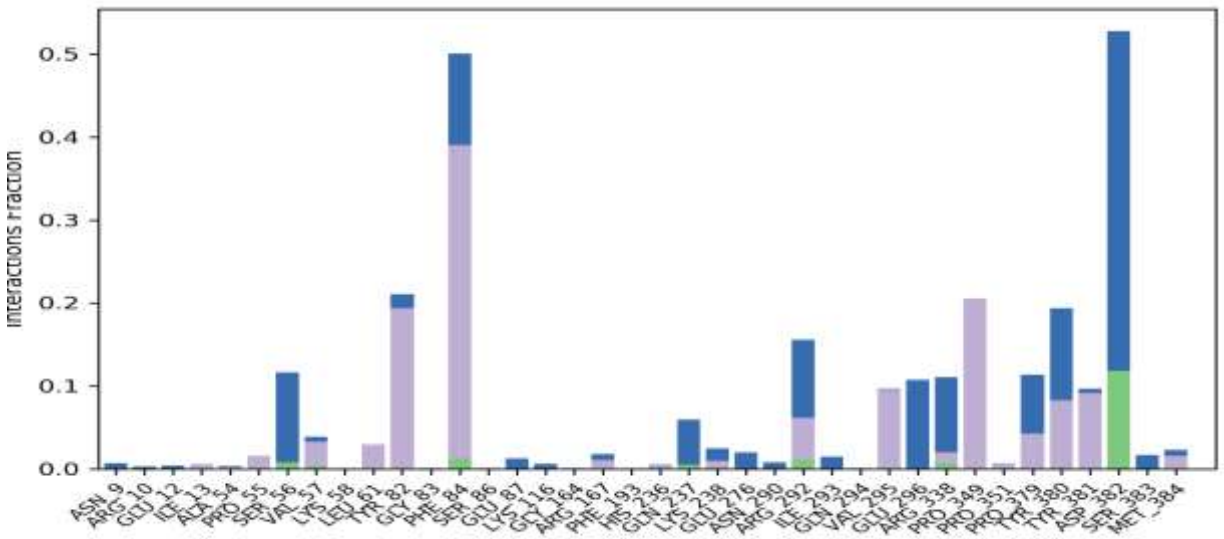

Figure 8: Protein-ligand contact histogram (3jzi)

Discussion

Herbicide that produces resistance have been classified into further two different categories, tar- get site resistance and non-target site resistance. Herbicides are very efficient weed control tech- niques that have been used in agricultural as long as no-till farming technique was introduced (Naylor, 2008). These herbicides are used to control the selectively grass weed on the plant of dicot. The irreversible dependent enzymes that block the inhibitors of the ACCase that catalyzes the synthesis pathway of fatty acid (Dayan et.al., 2019). Furthermore, to check their interaction against the weedicides and for their early detection to perform the Docking and Simulation analysis.

Protein ligand interaction and simulation analysis:

This novel study result indicates that the ACCase of 3jzf protein bind to the Fenoxaprop-p ethyl in Auto dock vina and visualize in Discovery studio and simulation analysis was done on Desmond Schrodinger. The 3jzf protein bind with the ARG_292 and make good interaction, the HIS_209 make Hydrophobic bond, GLN_233 and GLN_237 make good hydro- gen bond and HIS_236 make water bridges. These residues make excellent interaction with the surrounding residues in 3jzf protein with the ligand Fenoxaprop-p ethyl, ASP_382 is the most important ones in terms of H-bonds for (3jzi) that is not stable bonding. there more the protein of 3jzi has no interaction with the ligand Fenoxaprop-p ethyl.

The complex 3jzf reveals that the complex reaches stability at 5 ns and remains stable until 35 ns, after which the RMD of the ligand increases somewhat but again becomes stable with protein. The RMSD plot of the complex 3jzi shows that it reaches stability about 30 ns. However, the RMSD for the ligand is quite high, indicating a poor interaction. After then, an average RMSD value of 2.0 for (3jzf) and 3.0 for (3jzi) remains for ligand up to 50 ns. After becoming stable, the RMSD of proteins varies within 1.0 Angstrom. This indicates that the ligand stayed attached to the receptor's binding site for most of the simulation time. However, there is greater variation in (3jzi) than in (3jzf).

This present workflow for the diagnosis of the weedicides in the field of agriculture to overcome the loss. This is the novel study in this filed because, at the early stage no one perform these proteins (3jzf and 3jzi) and ligand (Fenoxaprop-p-ethyl) interaction for the early detection of the binding and active site. In results we get the general information about the physical properties of the atom. So, that will be helpful for the betterment and better yield from the field. in the agriculture area.

Conclusion:

In this molecular docking study of protein ligand interaction of the ACCase enzyme that have two proteins of 3jzf and 3jzi which have been attain from the Data Bank of protein (PDB), and herbicide Fenoxaprop-p ethyl as ligand were retrieved from PubChem database. ACCase used as an active site and Fenoxaprop-p ethyl used as a binding site. Docking analysis was done by using Auto Dock Vina which employs an iterative local search method Binding energies (Kcal/mol) and optimal binding conformations were obtained consequently. In Dis- covery Studio, the lowest energy coefficients of the binding confirmations were chosen then displayed. To discover the protein-ligand interaction implicated in the amino acids, linear (2D) and spatial (3D) interaction plots were examined.

Molecular dynamics simulations were run for 50 nanoseconds using Desmond, a Schrö- dinger LLC package. Docking experiments provided the earliest step of protein and ligand complexes for molecular dynamics modelling. In static circumstances, Molecular Docking Studies predict ligand binding condition. To anticipate the physiological environment in the ligand binding status, simulations were performed. Protein Preparation Wizard or Maestro were used to create protein–ligand complexes. It includes sophisticated optimization and reduction. The Desmond simulation's routes were investigated. MD trajectory analysis was used to calcu- late the interaction of protein–ligand RMSD, and RMSF. A result of 1.0 means that the target contact was maintained throughout the simulation. Because certain protein residues may form numerous interactions of the same subtype with the ligand, values greater than 1.0 are possible.

Furthermore, the result concluded that the ACCase of 3jzf protein bind to the Fenoxa- prop-p ethyl in Auto dock vina and visualize in Discovery studio and simulation analysis was done on Desmond Schrodinger. The 3jzf protein bind with the ARG_292 and make good in- teraction, the HIS_209 make Hydrophobic bond, GLN_233 and GLN_237 make good hydro- gen bond and HIS_236 make water bridges. These residues make excellent interaction with the surrounding residues in 3jzf protein with the ligand Fenoxaprop-p ethyl, ASP_382 is the most important ones in terms of H-bonds for (3jzi) that is not stable bonding. there more the protein of 3jzi has no interaction with the ligand Fenoxaprop-p ethyl.

In future, this research is very helpful and strengthens the strategies development at molecular level to in to control the weedicide at early. as well as also detect the active and binding site, receptor ligand interaction and also make drug designing for the enhancement of the weedicide.

Practically, by this research target based specific protein-ligand interaction to suggest the specific resistance by weedicide.

References

Bo AB, Won OJ, Sin HT, Lee JJ, Park KW. 2017. Mechanisms of herbicide resistance in weeds. Korean Journal of Agricultural Science. 44:1–15.

Délye, C. 2013. Unravelling the genetic bases of non-target-site-based resistance (NTSR) to herbicides: A major challenge for weed science in the forthcoming decade. Pest Manag. Sci. 69, 176–187.

Délye, C. Jasieniuk, M.; Le Corre. 2013. V. Deciphering the evolution of herbicide resistance in weeds. Trends Genet. 29, 649–658.

Gaines, T.A. Zhang, W. Wang, D. Bukun, B. Chisholm, S.T. Shaner, D.L. Nissen, S.J. Patzoldt, W.L. Tranel, P.J. Culpepper, A.S. et al. 2010. Gene amplification confers glyphosate resistance in Amaranthus palmeri. Proc. Natl. Acad. Sci. USA 107, 1029–1034.

Hirschberg, J. Mcintosh, L. 1983. Molecular basis of herbicide resistance in Amaranthus hybridus. Science 222, 1346–1349.

Kudsk P, Streibig JC. 2003. Herbicides – a two-edged sword. Weed Res. 43:90–102.

Kaundun, S.S., S. Hutchings, R.P. Dale, and E. Mcindoe. 2012. Broad Resistance to ACCase Inhibiting Herbicides in a Ryegrass Population Is Due Only to a Cysteine to Arginine Mutation in the Target Enzyme. 7(6): 1–9. doi: 10.1371/journal.pone.0039759.

Kim, S., Chen, J., Cheng, T., Gindulyte, A., He, J., He, S., Li, Q., Shoemaker, B. A., Thiessen, P. A., Yu, B., Zaslavsky, L., Zhang, J., & Bolton, E. E. (2019). PubChem in 2021: new data content and improved web interfaces. Nucleic acids research, 49(D1), D1388–D1395

Kukorelli, G., P. Reisinger, and G. Pinke. 2013. ACCase inhibitor herbicides – selectivity , weed resistance and fitness cost : a review. Int. J. Pest Manag. 59(3): 165–173. doi: 10.1080/09670874.2013.821212.

Laforest, M., Soufiane, B., Simard, M., Obeid, K., Page, E., and Nurse, R. E. 2017. Acetyl-CoA carboxylase overexpression in herbicide-resistant large crabgrass (Digitaria sanguinalis). Pest. Manag. Sci. 73, 2227–2235. doi: 10.1002/ps. 4675

Laforest, M. Soufiane, B. Simard, M.J. Obeid, K. Page, E. Nurse, R.E. 2017. Acetyl-CoA carboxylase overexpression in herbicide-resistant large crabgrass (Digitaria sanguinalis). Pest Manag. Sci. 73, 2227–2235.

Markowetz, F. 2017. All biology is computational biology. PLoS Biol 15(3): e2002050.
Moss, S. R. 2002. Herbicide-resistant weeds. In: Naylor REL, editor. Weed management handbook. Oxford: Blackwell Science. p. 225–252.
National Center for Biotechnology Information (2021). PubChem Compound Summary for CID 47938, Fenoxaprop-ethyl. Retrieved April 3, 2021
Powles, S.B. Yu, Q. 2010. Evolution in action: Plants resistant to herbicides. Ann. Rev. Plant Biol. 61, 317–347.
Takano, H.K., R. Fernando, L. Ovejero, G.G. Belchior, G. Potrich, et al. 2021. ACCase-inhibiting herbicides: mechanism of action, resistance evolution and stewardship. : 1–11.
Wan, H., Sjölinder, M., Schairer, H. U., and Leclerque, A. 2004. A new dominant selection marker for transformation of Pichia pastoris, to soraphen A resistance. J. Microbiol. Meth. 57, 33–39. doi: 10.1016/j.mimet.2003.11.013.
Yang, X., Guschina, I. A., and Hurst, S. 2018. The action of herbicides on fatty acid biosynthesis and elongation in barley and cucumber. Pest. Manag. Sci. 66, 794–800. doi: 10.1002/ps.1944 Powles, S. B. 2005. Molecular bases for sensitivity to acetyl-coenzyme a carboxylase inhibitor in black-grass. Plant Physiol. 137, 794–806. doi: 10.1104/ pp.104.046144t.
Ye, F., P. Ma, Y.Y. Zhang, P. Li, F. Yang, et al. 2018. Herbicidal activity and molecular docking study of novel accase inhibitors. Front. Plant Sci. doi: 10.3389/fpls.2018.01850.